Static-light $\bar{Q}\bar{Q}qq$ potentials with u, d, s from Lattice QCD

Excited QCD 2026 , University of Granada, Carmen de la Victoria, 8-14 January

Pedro Bicudo [1a], Marina Krstic Marinkovic [2b], Lasse Müller [3c], **Bernardo Picão** [1d], Marc Wagner [4e]

[1] CeFEMA, Univ. Lisboa, Portugal; [2] ITP, ETH Zürich, Switzerland; [3] ITP and [4] HRA Hesse for FAIR, Univ. Frankfurt, Germany

[a] *bicudo@tecnico.ulisboa.pt,* [b] *marinama@ethz.ch,* [c] *lmueller@itp.uni-frankfurt.de,* [d] *bernardo.picao@tecnico.ulisboa.pt,* [e] *mwagner@itp.uni-frankfurt.de*

January 11, 2026

Motivation: the Narrow Heavy Multiquark States...

- Jean-Marc Richard, J. P. Ader, J. M. Richard and P. Taxil, Phys. Rev. D **25**, 2370 (1982) , anticipated that tetraquarks would bind if they would have two light quarks and two heavy antiquarks, and in 2021 the T_{cc} with flavor $ud\bar{c}\bar{c}$ was finally observed at LHCb.

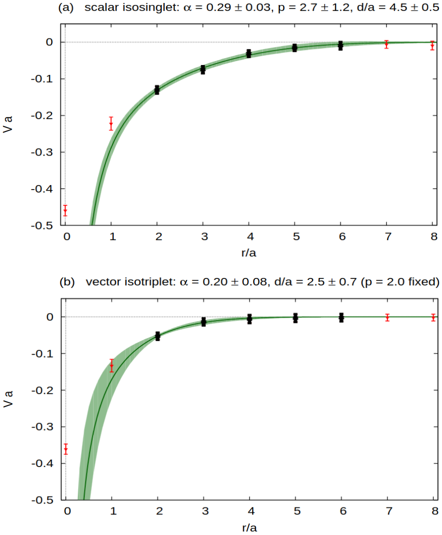

Attractive $\bar{Q}\bar{Q}qq$ potentials from

M. Wagner "Forces between static-light mesons," PoS **LATTICE2010**, 162 (2010) [arXiv:1008.1538 [hep-lat]].

P. Bicudo and M. Wagner, "Lattice QCD signal for a bottom-bottom tetraquark," Phys. Rev. D **87**, no.11, 114511 (2013)

with chiral extrapolation and improved plateau fits δmass $= -90 \pm 43$ MeV.

P. Bicudo, K. Cichy, A. Peters, B. Wagenbach and M. Wagner, Phys. Rev. D **92**, no.1, 014507 (2015).

T_{bbs} and T_{bc} are close to binding but T_{cc} is farther. However spin effects decrease the binding by 30 %.

There is a tension with the lattice computations with NRQCD who find more binding ($E_B > 100$ MeV)!

Motivation: A Bridge to Nuclear Physics

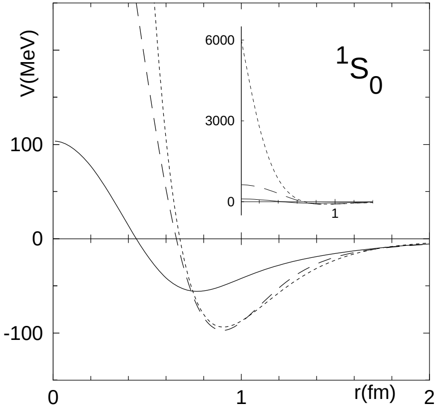

Example of N − N potentials for n − p

V. G. J. Stoks, R. A. M. Klomp, C. P. F. Terheggen and J. J. de Swart, "Construction of high quality N N potential models," Phys. Rev. C **49**, 2950-2962 (1994)

Meson exchange may produce small bumps, with opposite sign to the main part, in our potentials.

Each static-light meson has:
I=1/2, S=1/2, colour=1,
the same quantum numbers of a nucleon *N*.

Our potentials are qualitatively similar to the nucleon-nucleon (N-N) interaction, fundamental to nuclear physics. At large distances we might then expect the presence of the one pion exchange (OPE) potential.

Lattice Setup: Tetraquark Interpolators and Correlators

- Interpolator for $\bar{b}\bar{b}ud$ (assuming isospin symmetry):

$$\mathcal{O}^{I,\Gamma}(\mathbf{r}_1, \mathbf{r}_2) \quad = (\mathcal{C}\Gamma)_{AB} \left(\mathcal{C}\tilde{\Gamma}\right)_{CD} \left(\bar{b}^a_C(\mathbf{r}_1) u^a_A(\mathbf{r}_1)\, \bar{b}^b_D(\mathbf{r}_2) d^b_B(\mathbf{r}_2) \mp (u \leftrightarrow d)\right), \tag{1}$$

- Correlation function:

$$\begin{aligned}
\mathcal{C}^{I,\Gamma}(\mathbf{r}_2 - \mathbf{r}_1, t_2 - t_1) &= \langle \Omega | \mathcal{O}^{I,\Gamma\,\dagger}(\mathbf{r}_1, \mathbf{r}_2; t_2) \mathcal{O}^{I,\Gamma}(\mathbf{r}_1, \mathbf{r}_2; t_1) | \Omega \rangle \\
&\propto \Big\langle \left(\gamma_0 \Gamma^\dagger \gamma_0\right)_{BA} \Gamma_{CD} \Big(\mathrm{Tr}_c \Big[U(\mathbf{r}_1, t_2; \mathbf{r}_1, t_1) \left(M_q^{-1}\right)_{CA} (\mathbf{r}_1, t_1; \mathbf{r}_1, t_2) \Big] \\
&\quad \times \mathrm{Tr}_c \Big[U(\mathbf{r}_2, t_2; \mathbf{r}_2, t_1) \left(M_q^{-1}\right)_{DB} (\mathbf{r}_2, t_1; \mathbf{r}_2, t_2) \Big] \\
&\quad \pm \mathrm{Tr}_c \Big[U(\mathbf{r}_1, t_2; \mathbf{r}_1, t_1) \left(M_q^{-1}\right)_{CA} (\mathbf{r}_1, t_1; \mathbf{r}_2, t_2)\, U(\mathbf{r}_2, t_2; \mathbf{r}_2, t_1) \left(M_q^{-1}\right)_{DB} (\mathbf{r}_2, t_1; \mathbf{r}_1, t_2) \Big] \Big) \Big\rangle
\end{aligned}$$

$\equiv$ 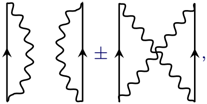 , (2)

- Normalize with B-meson correlator

$$\frac{\mathcal{C}^{I,\Gamma}(\mathbf{r}, t)}{\mathcal{C}_1(t)\mathcal{C}_2(t)} \xrightarrow[t \to \infty]{} A \exp\left(-\left(V^{I,\Gamma}(\mathbf{r}) - (m_1 + m_2)\right) t\right), \tag{3}$$

- $\bar{b}\bar{b}us$ correlator: interpolator corresponds to Eqn. 1 with $d \to s$, different light quarks produce 4 diagrams instead of 2:

$\mathcal{C}^{\Gamma}_s(\mathbf{r}_2 - \mathbf{r}_1, t_2 - t_1) \equiv$ 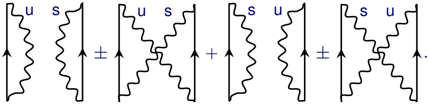

. (4)

Lattice Setup: Symmetries and Quantum Numbers

	$I=0$		$I=1$	
Γ	$\lvert j_z\rvert, \mathcal{P}, \mathcal{P}_x$	shape	$\lvert j_z\rvert, \mathcal{P}, \mathcal{P}_x$	shape
$\gamma_5 + \gamma_0\gamma_5$	$0, -+$	A,SS	$0, ++$	R,SS
1	$0, +-$	A,SP	$0, --$	R,SP
γ_0	$0, --$	R,SP	$0, +-$	A,SP
$\gamma_5 - \gamma_0\gamma_5$	$0, -+$	A,PP	$0, ++$	R,PP
$\gamma_3 + \gamma_0\gamma_3$	$0, +-$	R,SS	$0, --$	A,SS
$\gamma_3\gamma_5$	$0, ++$	A,SP	$0, -+$	R,SP
$\gamma_0\gamma_3\gamma_5$	$0, -+$	R,SP	$0, ++$	A,SP
$\gamma_3 - \gamma_0\gamma_3$	$0, +-$	R,PP	$0, --$	A,PP
$\gamma_{1/2} + \gamma_0\gamma_{1/2}$	$1, +(+/-)$	R,SS	$1, -(+/-)$	A,SS
$\gamma_{1/2}\gamma_5$	$1, +(-/+)$	A,SP	$1, -(-/+)$	R,SP
$\gamma_0\gamma_{1/2}\gamma_5$	$1, -(-/+)$	R,SP	$1, +(-/+)$	A,SP
$\gamma_{1/2} - \gamma_0\gamma_{1/2}$	$1, +(+/-)$	R,PP	$1, -(+/-)$	A,PP

Quantum numbers and properties of the resulting $\bar{b}\bar{b}ud$ potentials:
A = attractive, R = repulsive; SS, SP ,PP = asymptotic value $2m_B$, $m_B + m_{B_0^*}$, $2m_{B_0^*}$.

Quantum numbers:

- $\lvert j_z\rvert$: angular momentum in separation direction;
- $\mathcal{P}$: Behavior under parity;
- $\mathcal{P}_x$: Behavior under reflection along an axis perpendicular to the separation axis.

Lattice Setup: Details of the Calculation

ensemble	T/a	L/a	a[fm]	m_π[MeV]	N_{cfg}	α_{APE}	n_{APE}	κ_G	n_G
A5	64	32	0.0755	331	100	0.5	30	0.5	50
N6	96	48	0.0486	340	50	0.5	50	0.5	120
G8	128	64	0.0658	185	30	0.5	35	0.5	70

CLS ensembles with 2 flavors of improved Wilson fermions.

- Our computations use the openQ*D codebase, a modern and versatile repository for CPU parallelization in LQCD I. Campos *et al.* [RC*], Eur. Phys. J. C **80**, no.3, 195 (2020)
- We employ stochastic timeslice-to-all propagators using 12 sources per timeslice on 6 (N6) and 8 (A5, G8) timeslices per configuration, respectively.

$$\frac{1}{N}\sum_{n=1}^{N}\phi^a_\alpha(t_1,\boldsymbol{x})[t_0,n]\left(\eta^b_\beta(t_2,\boldsymbol{y})[t_0,n]\right)^\dagger = (D^{-1})^{ab}_{\alpha\beta}(\boldsymbol{x};\boldsymbol{y},t_0) + \mathcal{O}(N^{-\alpha}) \quad (5)$$

- We apply APE smearing to the gauge fields and Gaussian smearing to the source and sink, as well as the HYP2 static action. The algorithms and notation are consistent with K. Jansen *et al.* [ETM], JHEP **12**, 058 (2008).
- We define an improved separation to replace the lattice distance, which reduces discretization errors at small scales:

$$\mathbf{r}_{lat} \to \mathbf{r}_{impr} = \frac{4\pi a}{G\left(\frac{\mathbf{r}}{a}\right)}. \quad (6)$$

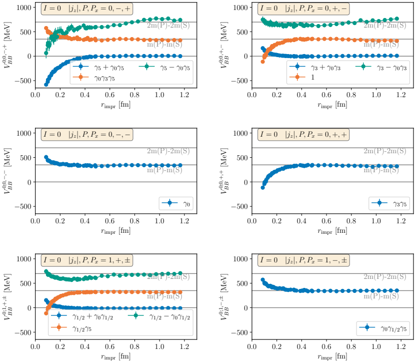

$\bar{b}\bar{b}ud$ *potentials for* $I = 0$*, ensemble N6.*

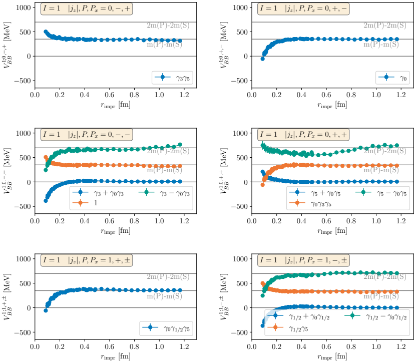

$\bar{b}\bar{b}ud$ *potentials for* $I = 1$*, ensemble N6.*

- On-axis separations up to $|\mathbf{r}| = 1.2$ fm;
- All possible off-axis separations are included at shorter distances;
- 24 independent creation operators dictated by the Γs;
- No correlation matrices → excited potentials might be contaminated by lower potentials.

Results: Potentials $I = 0$ and $I = 1$ with Lowest Asymptotic Value

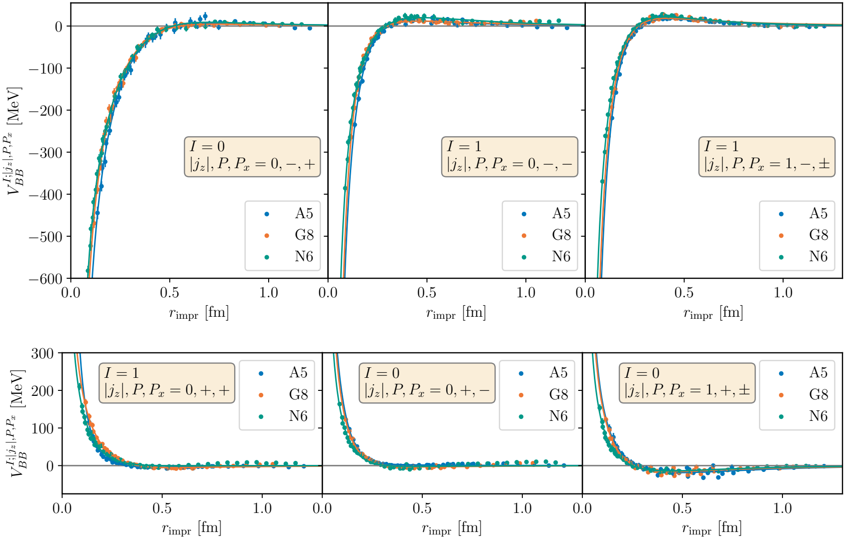

All attractive and repulsive potentials with asymptotic value of $2m_S$ for ensembles A5, G8 and N6.

Results: Phenomenological Analysis

In the quark model, the potential for the two light or the two heavy quarks has the structure:

- Leading, color dependent $\frac{\boldsymbol{\lambda}^1 \cdot \boldsymbol{\lambda}^2}{\boldsymbol{\lambda} \cdot \boldsymbol{\lambda}}$: for **3** it equals $-\frac{1}{2}$ thus attractive, whereas for $\bar{\mathbf{6}}$ it equals $\frac{1}{4}$ and is repulsive;
- next to leading (hyperfine) $\frac{\boldsymbol{\lambda}^1 \cdot \boldsymbol{\lambda}^2}{\boldsymbol{\lambda} \cdot \boldsymbol{\lambda}}$ $(-\boldsymbol{\sigma}^1 \cdot \boldsymbol{\sigma}^2)$: factor of 3 (stronger) for $S = 0$ and -1 (weaker) for $S = 1$,
- At short distances, has a OGE Coulomb potential: $\frac{\boldsymbol{\lambda}^1 \cdot \boldsymbol{\lambda}^2}{\boldsymbol{\lambda} \cdot \boldsymbol{\lambda}} \frac{\alpha}{r}$.

  $\Longrightarrow$ Consistent with the observation that the "good" scalar-isoscalar diquark is more attractive than the "bad" vector-isovector diquark. Antisymmetry then enforces the flavor wavefunctions ($\bar{\mathbf{3}}$ and **6**, resp.).
- At intermediate distances we have two static-light mesons, and the potentials are screened with a factor proportional to the static-light wave-function ϕ^2, typically an Airy function or Gaussian with exponent $p = 1.5$ to 2.

  $\Longrightarrow$ This leads to a simple ansatz, where C depends on the light quarks and includes medium range effects:

$$V(r) = \left(\frac{\boldsymbol{\lambda}^1 \cdot \boldsymbol{\lambda}^2}{\boldsymbol{\lambda} \cdot \lambda}_{\mathrm{H}} \frac{\alpha}{r} + C \right) \exp\left[- \left(\frac{r}{d} \right)^p \right] \tag{7}$$

At large distances, we have meson exchanges, in particular the one pion exchange (OPE) potential:

- OPE includes a hyperfine potential $(\boldsymbol{\tau}_1 \cdot \boldsymbol{\tau}_2)(\boldsymbol{\sigma}_1 \cdot \sigma_2) \left[\frac{e^{-m_\pi r}}{r} + \cdots \right]$ which, due to the Pauli principle, is opposed to the dominant quark model term $\frac{\boldsymbol{\lambda}^1 \cdot \boldsymbol{\lambda}^2}{\boldsymbol{\lambda} \cdot \boldsymbol{\lambda}}$, producing an opposite bump at large distances.
- However, the main signature is the tensor part: $(\boldsymbol{\tau}_1 \cdot \boldsymbol{\tau}_2)[(\boldsymbol{\sigma}_1 \cdot \boldsymbol{r})(\boldsymbol{\sigma}_2 \cdot \boldsymbol{r}) + \cdots] \left[\frac{e^{-m_\pi r}}{r} + \cdots \right]$

  $\hookrightarrow$ in our case $(\boldsymbol{\sigma}_1 \cdot \hat{z})(\boldsymbol{\sigma}_2 \cdot \hat{z})$ is $= -1$ for $j_z = 0$ and is $+1$ for $|j_z| = 1$.

$\bar{Q}\bar{Q}qq$	Ens.	α_1	d[fm]	p	c [MeV]	E_B[MeV]
$\bar{b}\bar{b}ud$	A5	0.436(0.024)	0.570(0.064)	1.99(0.337)	164(19)	60(12)
	G8	0.359(0.012)	0.552(0.067)	2.28(0.74)	130(16)	20(5)
	N6	0.271(0.074)	0.349(0.029)	2.93(0.77)	19(53)	12(5)
$\bar{b}\bar{b}us$	A5	0.414(0.017)	0.468(0.027)	1.70(0.23)	156(6)	no binding
	G8	0.404(0.014)	0.409(0.019)	1.28(0.11)	157(6)	5(2)
	N6	0.290(0.004)	0.612(0.040)	2.14(0.26)	107(5)	no binding

Fitting parameters of our ansätze for the $\bar{b}\bar{b}ud$ and $\bar{b}\bar{b}us$ potentials, and binding energies for T_{bb} and T_{bbs} in the Born-Oppenheimer approximation.

- Notice, with the C parameter, the screening in the isoscalar case is close to a Gaussian.
- We achieve a larger significance than with the 2010 and 2015 potentials.
- However, the E_B are in general similar to the ones of the 2010 potential, with no binding for T_{bc} and T_{cc}.
- Besides, the different ensembles show rather different fits, visible in the different binding energies.

Analysis: the bumps from good and bad diquarks

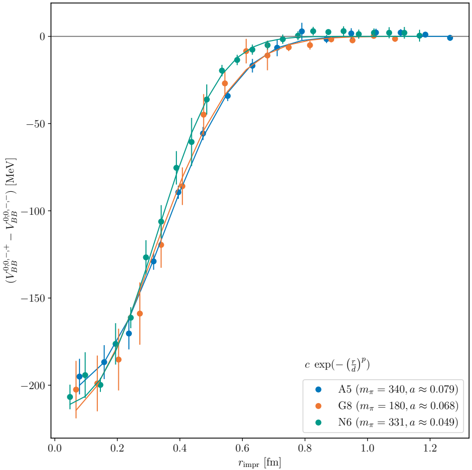

Difference between the "good" $I = 0$ and $|j_z|, P, P_x = 0, -, +$ and "bad" $I = 1$ and $|j_z|, P, P_x = 1, -, -$ computed with the ratio of the correlators.

Comparing with the study of "good" and "bad" diquarks in lattice QCD, for instance in Ref. A. Francis, P. de Forcrand, R. Lewis and K. Maltman, JHEP **05**, 062 (2022) , we verify this difference to tend to the diquark mass difference $\simeq$ 200 MeV, in the limit of vanishing distances.

Results: Analysis of the OPE Bump

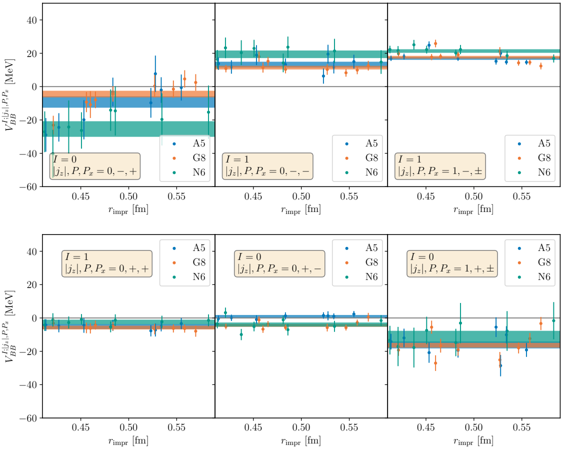

All attractive (top) and repulsive (bottom) potentials with the lowest asymptotic value of $2m_S$ for ensembles A5, G8 and N6 for intermediate separations $0.4 < r_{imp} < 0.6$.

- In this figure, the tensor interaction from OPE is expected shifts the center panel potentials with $|j_z| = 0$ from the right panel potentials with $|j_z| = 1$ ones (width of the line indicates one standard deviation).

Outlook: improve systematic errors in EMPs

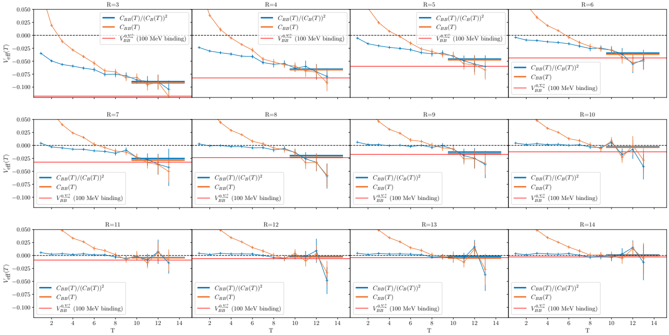

EMPs for our most attractive 'good' scalar-isoscalar potential.

- Clearly, our EMPs at short distances did not properly converge before the error bars get too large. This systematic error weakens the potential, and creates a tension with the NRQCD results.
  $\Longrightarrow$ We will increase statistics with more configurations soon!
  $\Longrightarrow$ Also utilize better smearings, like Wilson flow.
  $\Longrightarrow$ Mainly, we will compute the correlation matrix to decrease the excited state contamination of the plateaux.
- When dividing the 'good' and 'bad' most attractive potentials, the short range effects are under control:

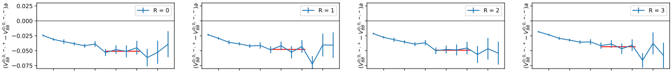

Conclusion and Further Prospects

- We improve on our long-established results with new CLS ensembles including a pion not far from physical, by employing CPU parallelization using the OpenQ*D codebase, and by taking into account off-axis separations.
- We study 24 operators, for $I = 0$, $I = 1$ and $s = 1$, for the asymptotic masses $2m_S$, $m_S + m_P$ and $2m_P$.
- We provide a robust phenomenological description of the calculated potentials: OGE at short distances, at intermediate distances there is screening of the static-light wavefunction, and at large separations, the presence of bumps due to the spin-dependent hyperfine interactions between the constituent light quarks, as expected from the quark models, as well as a tentative evidence for the long distance One Pion Exchange (OPE) potential, with its spin-dependent tensorial signature.
- Our analysis matches the recent results of I. Vujmilovic, S. Prelovsek et al., arXiv:2510.17549 [hep-lat] (2025) that use EM form factors to establish that the internal structure of the T_{bb} is composed of one heavy diquark and one light antidiquark, and give a binding energy of $\sim 60 MeV$.
- **However**, more statistics and better control of the systematics are still needed. Our systematic errors still lead to less attractive potentials, our binding energies are smaller than the ones calculated with NRQCD bottom quarks on the lattice.
- Beyond extending to more configurations and performing the GEVP analysis with the dominant channels, we will also explore other smearing techniques.

THANK YOU !!!

Backup: Operators for $Q\bar{Q}qq$

$$
\mathcal{C}_{\bar{Q}Q\bar{l}l}(\mathbf{r}_1, t_1|\mathbf{r}_2, t_2)
= \begin{pmatrix} \left\langle \mathcal{O}_{\bar{Q}Q}(\mathbf{r}_1,\mathbf{r}_2,t_1) \middle| \mathcal{O}_{\bar{Q}Q}(\mathbf{r}_1,\mathbf{r}_2,t_2) \right\rangle & \left\langle \mathcal{O}_{\bar{Q}Q\bar{l}l}(\mathbf{r}_1,\mathbf{r}_2,t_1) \middle| \mathcal{O}_{\bar{Q}Q}(\mathbf{r}_1,\mathbf{r}_2,t_2) \right\rangle \\ \left\langle \mathcal{O}_{\bar{Q}Q}(\mathbf{r}_1,\mathbf{r}_2,t_1) \middle| \mathcal{O}_{\bar{Q}Q\bar{l}l}(\mathbf{r}_1,\mathbf{r}_2,t_2) \right\rangle & \left\langle \mathcal{O}_{\bar{Q}Q\bar{l}l}(\mathbf{r}_1,\mathbf{r}_2,t_1) \middle| \mathcal{O}_{\bar{Q}Q\bar{l}l}(\mathbf{r}_1,\mathbf{r}_2,t_2) \right\rangle \end{pmatrix}
$$

$=$ 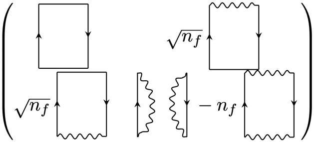

,

Correlation matrix for the QQ̄qq systems, including a quarkonium operator.

Backup: Symmetries and Quantum Numbers

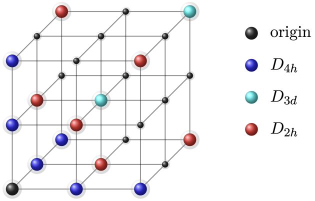

On and off-axis separations and corresponding symmetry groups.

Axis	Sym. Group	n_{rot}	$\|L\|$
$(0, 0, a)$	D_{4h}	4	$0, 4, 8, \ldots$ $1, 3, 5, \ldots$ $2, 6, 10, \ldots$
(a, a, a)	D_{3d}	3	$0, 3, 6, \ldots$ $1, 2, 4, \ldots$
$(0, a, a)$	D_{2h}	2	$0, 2, 4, \ldots$ $1, 3, 5, \ldots$
$(0, a, b)$ (a, a, b)	S_4	1	$0, 1, 2, \ldots$
(a, b, c)	C_1	1	$0, 1, 2, \ldots$

Backup: potentials with $s = 1$ and lowest asymptotic value $2m_S$.

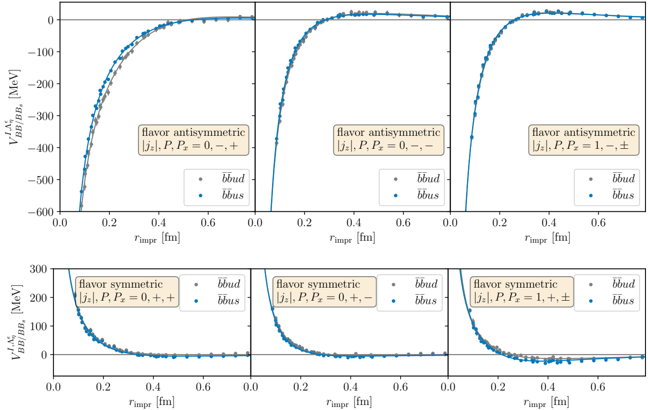

All attractive and repulsive $\bar{b}\bar{b}us$ potentials with asymptotic value $2m_S$, for ensemble N6. The gray data points and fits indicate corresponding results for $\bar{b}\bar{b}ud$.

Backup: Results for Different Separations

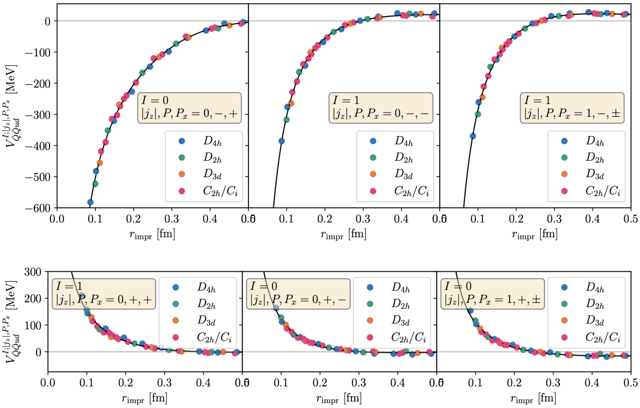

All attractive (top) and repulsive (bottom) $\bar{Q}\bar{Q}ud$ potentials with the lowest asymptotic value of $2m_S$ for ensemble N6. Different symmetry groups D_{4h}, D_{2h}, D_{3d}, C_{2h} and C_i of separations are indicated by separate colors.

Backup: Fit of the Coulomb Potential

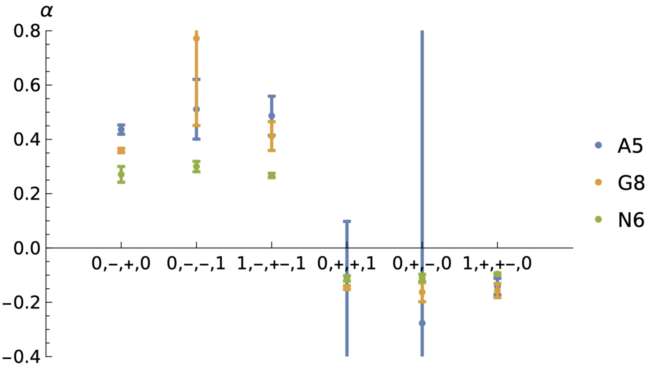

The Coulomb parameter α of the central potential fitted from the ensembles.